ELSEVIER

Journal of Magnetism and Magnetic Materials 239 (2002) 351–355

Journal of magnetism and magnetic materials

www.elsevier.com/locate/jmmm

Magnetically induced second harmonic generation (MSHG) as a tool for the studies of surface magnetism

Katsuaki Sato[a,*], Koki Takanashi[b], Kiyokazu Himi[b], Andrei Kirilyuk[c], Theo Rasing[c]

[a] *Department of Applied Physics, Faculty of Technology, Tokyo University of Agriculture and Technology, 2-24-16 Nakacho, Koganei, Tokyo 184-8588, Japan*

[b] *Institute for Material Research, Tohoku University, Sendai, Miyagi 980-8577, Japan*

[c] *Research Institute for Materials, University of Nijmegen, 6525 ED Nijmegen, The Netherlands*

Abstract

Nonlinear magneto-optical effect is a powerful tool for investigation of magnetism at the surfaces and interfaces of magnetic materials, particularly superlattices and multilayers. In this paper we introduce our studies on the magnetically induced second harmonic generation (MSHG) and nonlinear magneto-optical Kerr rotation observed in epitaxial superlattices of Fe/Au(0 0 1) and Co/Ru(0 0 0 1).

Keywords: Nonlinear magneto-optical effect; Surface magnetism; Second harmonic generation; Superlattices

Recently, nonlinear magneto-optical effect is attracting attention as a novel tool for investigation of surfaces and interfaces in magnetic materials. Among different kinds of nonlinear magneto-optical effects, the most intensively studied is the magnetic second harmonic generation (MSHG) [1]. This effect is known to be very sensitive to surfaces and interfaces, since the electric dipole-induced SHG in the materials with an inversion symmetry becomes allowed only at surfaces and interfaces where an inversion symmetry is broken. In addition, the magnetization also lowers the symmetry at the surfaces and interfaces. This is the reason why MSHG has been applied to studies of magnetic superlattices and multilayers [2,3]. It was revealed from the studies on Co/Au multilayers that MSHG intensity depends clearly on the number of interfaces [4]. On the other hand, MSHG experiments on a 10 ML Cu/Co(x ML)/Cu(0 0 1) system with varying Co thickness revealed that a magnetization contrast of MSHG defined by $\{I(+M) - I(-M)\}/\{I(+M) + I(-M)\}$, where $I(\pm M)$ is second harmonic output for $\pm M$ (two opposite magnetization directions), increases monotonously with Co layer thickness, in accordance with a multiple reflection model [5].

In this study we have applied the MSHG technique to Fe/Au and Co/Ru superlattices prepared on MgO or Al_2O_3 substrates with atomically controlled epitaxial layers. The superlattice with a modulation of mono-atomic layers of Fe and Au has been known to show an artificial order with an $L1_0$ structure that does not exist in nature [6]. Such an artificial structure remains at interfaces between Fe and Au layers even for the modulation period longer than mono-atomic layer [7]. The linear magneto-optical spectra of the superlattices modulated by integer and non-integer numbers of atomic layers have been studied intensively, suggesting a formation of the band structure peculiar to the artificial structure [8,9]. While the Fe/Au superlattices show uniform ferromagnetic structure for short modulation periods, Co/Ru(0 0 0 1) superlattices are subjected to strong antiferromagnetic coupling between Co layers, which leads to an artificial antiferromagnet in some cases [10]. Recently, good epitaxial growth of Co/Ru superlattice was realized and linear magneto-optical

*Corresponding author. Tel.: +81-423-88-7120; fax: +81-423-87-8151.

E-mail address: satokats@cc.tuat.ac.jp (K. Sato).

0304-8853/02/$ - see front matter
PII: S0304-8853(01)00599-6

Kerr experiments were carried out. The measured linear Kerr rotation angle of Co(5 ML)/Ru(5 ML) superlattice was almost ten times smaller than that of HCP Co, which was successfully explained from the first-principle band theory [11].

Strong second harmonic (SH) signals were observed from both Fe/Au and Co/Ru superlattices. In Fe/Au superlattices, a clear four-fold symmetry was observed in the azimuthal dependence of SH intensity and nonlinear Kerr rotation. On the other hand, only an isotropic azimuthal dependence of SH signals was observed from the Co/Ru superlattice.

The specimens of Fe(x ML)/Au(x ML) superlattices used in the present study are the same ones as used in the previous linear magneto-optical studies [9]. They were prepared on MgO(1 0 0) substrates by an ultra high vacuum (UHV) deposition technique. The base pressure of the deposition system was 3×10^{-10} Torr. An Fe seed layer of 1 nm followed by a Au buffer layer of 50 nm was deposited at 200°C and subsequently annealed for 30 min to 1 h at 500°C. The orientation of the Au buffer layer was (0 0 1). Multilayers with N periods, each period consisting of x ML Fe and x ML Au, were deposited in the UHV system at 70°C on the Au buffer. The parameter x took either integer values or non-integer values between 1 and 4. Superlattice with $x = 15$ was employed for the nonlinear magneto-optical measurement. The axis of easy magnetization was in plane along the surface. As a typical example of non-integer superlattices, a sample with $x = 3.5$ is also studied. Details of preparation techniques were described elsewhere [12]. Formation of superlattice structure was confirmed by X-ray diffraction as described in detail in Ref. [9].

The Co(5 ML)/Ru(5 ML) superlattice was prepared on Ru(0 0 0 1) buffers deposited on a sapphire (1 1 $\bar{2}$ 0) substrate. Epitaxial growth was confirmed by RHEED observation. Details of preparation technique have been reported in the previous paper [13]. The magnetic anisotropy of the Co/Ru superlattice was perpendicular to the surface.

We used a mode-locked Ti-sapphire laser (Coherent, MIRA, $\lambda = 760$–810 nm) as a light source. The Ti-sapphire laser was excited by a 532-nm line of a 5-W diode-pumped YVO_4-SHG laser (Coherent, VERDI). The pulse width of the Ti-sapphire laser was 100–150 fs and the repetition rate was 80 MHz. The average power output of the laser was approximately 600 mW. To avoid sample damage by the laser irradiation, the average power of the light beam was reduced to $\frac{1}{10} - \frac{1}{20}$ of the original intensity using a rotating light chopper. The spot size of the laser beam focused on the sample was 40 μm in diameter and the peak power density was estimated as 0.5 GW/cm^2. The incident angle of the laser beam was fixed at 45° to the sample normal. A magnetic field up to about 0.3 T was applied in the longitudinal Kerr geometry, which was sufficient to saturate the Fe/Au superlattice, but not sufficient for the Co/Ru superlattice.

Sample was mounted on a computer-controlled rotating stage to obtain the azimuthal angle-dependence of the MSHG signal. The latter was measured for all the four combinations of input-output polarization; i.e., P_{in}–P_{out}, S_{in}–P_{out}, P_{in}–S_{out}, S_{in}–S_{out}, where the notations P and S denote the polarizations parallel and perpendicular to the incident plane of reflection, respectively. For measurements of the nonlinear Kerr rotation a computer-controlled rotating analyzer was employed.

The SHG light was effectively filtered using two blue filters (Hoya-Schott BG39) and guided to a photomultiplier (Hamamatsu R464), the output of which was guided to a preamplifier (Hamamatsu C5594) and a photon counting apparatus (Stanford Research SR400). Typical data-accumulation time was 10 s.

X-ray diffraction and electron diffraction analyses have elucidated that the Fe/Au superlattices follow the symmetry of MgO(0 0 1) substrate and have the 4/mmm symmetry for bulk and 4mm for surface. On the other hand, Co/Ru superelattices have the 6/mmm symmetry for bulk and 6mm for surface following the hexagonal symmetry of the Ru(0 0 0 1) buffer.

Fig. 1 shows typical polar plots of the azimuthal angle-dependence of the SH intensity for P_{in}–P_{out} configuration in samples of Fe (15 ML)/Au (15 ML) measured by rotating the sample [14]. In the figure, the open and the closed symbols represent those for two opposite directions of the magnetic field. Since the output signal from the photon counter was strong and free from data scattering, no further data processing was carried out. Well-defined four-fold symmetric pattern, which reflects the crystallographic symmetry (4/mmm) of the superlattice, was observed. Reversal of magnetization results in a rotation of the azimuthal pattern.

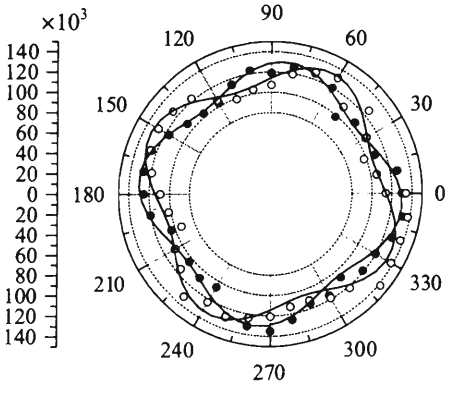

Fig. 1. Azimuthal angle dependence of SH intensity in Fe(15 ML)/Au(15 ML) superlattice.

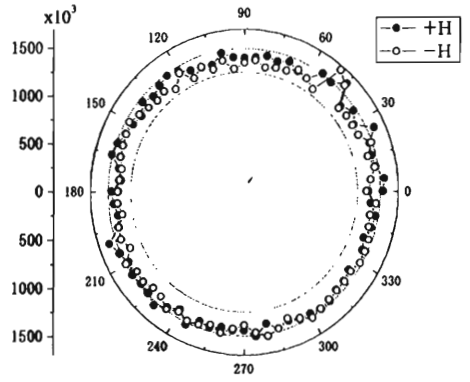

Fig. 2. Azimuthal angle dependence of Co(5 ML)/Ru(5 ML) superlattice.

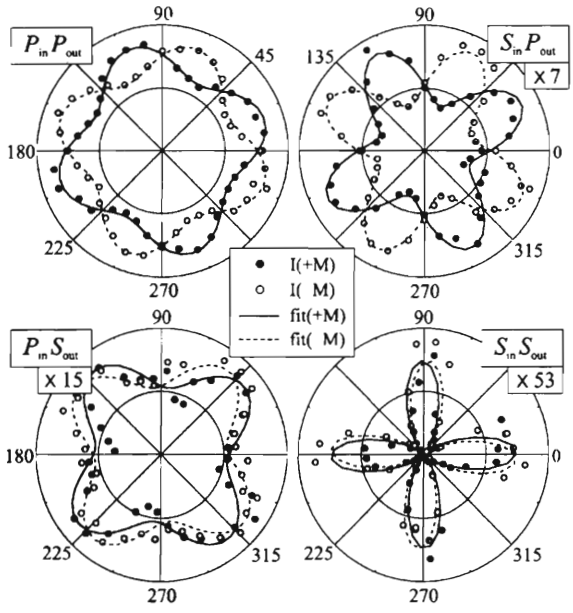

Fig. 3. Rotational anisotropy curves (experimental points and theoretical fits) of MSHG intensity in Fe(3.5 ML)/Au(3.5 ML) superlattice for all four polarization combinations. Multiplication factors by three plots show the scaling of the correspondingdata in order to reach the same intensity level as it is with Pin-Pout polarization combination.

On the other hand, as shown in Fig. 2, the polar plot of the azimuthal dependence of SH intensity in Co(5 ML)/Ru(5 ML) superlattice is isotropic, in spite of the six-fold symmetry of the c-plane of the HCP superlattice. Reversal of magnetic field yielded no change of the SH intensity.

In Fig. 3, the results of all four polarization combinations for the Fe(x ML)/Au(x ML) superlattice with $x = 3.5$ ML are plotted, for the longitudinal geometry. Note the different vertical scales for the various data, indicating a substantial difference for the MSHG response for different polarization combinations. It is also obvious that all data involving S_{in} or S_{out} polarization yield a much stronger anisotropy, which is a direct consequence of the in-plane xy tensor components that contribute to these signals. Even the weakest S_{in}–S_{out}-curve shows a clear four-fold symmetry pattern.

Azimuthal angle dependence of MSHG in superlattices has been analyzed theoretically in terms of the symmetric properties of nonlinear susceptibility tensor element. Usually, an analysis of MSHG results is performed assuming that the top surface and buried interfaces are the only sources of the nonlinear magneto-optical response. Their nonlinearity is described in terms of the effective surface/interface dipole-like nonlinear susceptibility $\chi^{(2)}_{ijk}(M)$, which is a third rank tensor. As will be described in more detail in our later publication [15], this contribution yields the following azimuthal patterns:

$$
\begin{aligned}
I^{ss}_{2\omega}(\varphi, \pm M) &= |\pm A^{ss} \pm B^{ss} \cos 4\varphi|^2,\\
I^{sp}_{2\omega}(\varphi, \pm M) &= |A^{sp} \pm C^{sp} \sin 4\varphi|^2,\\
I^{ps}_{2\omega}(\varphi, \pm M) &= |\pm A^{ps} \pm B^{ps} \cos 4\varphi|^2,\\
I^{pp}_{2\omega}(\varphi, \pm M) &= |A^{pp} \pm C^{pp} \sin 4\varphi|^2,
\end{aligned}
\tag{1}
$$

assuming that the effect in the magnetization is weak so that only the contributions of zeroth and first order in M should be accounted for. Here the $\pm$ sign stands in front of the magnetization-induced terms, which change sign upon magnetization reversal. Note that these patterns do not yield any effect of the magnetization reversal for S_{in}–S_{out} and P_{in}–S_{out} MSHG intensity in contrast to the experimental observation shown in Fig. 3. They are also unable to properly describe the patterns for the other two polarization combinations.

Therefore, one has to take into account additional anisotropic contributions to the second-order nonlinear response. In particular, the nonlocal (quadrupole-allowed) contribution from the bulk of a cubic nonmagnetic metals (Cu [16], Ag [17] and Al [18]) and semiconductors (Si [19]) has been shown to lead to a four-fold anisotropy of SHG at their (1 0 0) surfaces. This additional contribution from $\chi^{Q(2)}_{ijkl}$ modifies the rotational patterns to

$$
\begin{aligned}
I^{ss}_{2\omega}(\varphi, \pm M) &= |\pm A^{ss} \pm B^{ss} \cos 4\varphi + C^{ss} \sin 4\varphi|^2,\\
I^{sp}_{2\omega}(\varphi, \pm M) &= |A^{sp} + B^{sp} \cos 4\varphi \pm C^{sp} \sin 4\varphi|^2,\\
I^{ps}_{2\omega}(\varphi, \pm M) &= |\pm A^{ps} \pm B^{ps} \cos 4\varphi + C^{ps} \sin 4\varphi|^2,\\
I^{pp}_{2\omega}(\varphi, \pm M) &= |A^{pp} + B^{pp} \cos 4\varphi \pm C^{pp} \sin 4\varphi|^2.
\end{aligned}
\tag{2}
$$

Since, for our superlattice structures, the normal z direction is not equivalent to the tangential x, y directions, the symmetry of the interior is lower than cubic. Therefore, the analysis is performed for the 4/mmm symmetry. Eq. (2) was used for the theoretical fits

to the experimental data of Fig. 3, showing an excellent agreement between experiment and theory. In Table 1, an overview is given for the various fitting amplitudes used, indicating the relative strength of the various contributions. In some cases, the quality of the fit was noticeably improved by taking into account the complex character of the azimuthal amplitudes $A^{\alpha\beta}$, $B^{\alpha\beta}$ and $C^{\alpha\beta}$.

The fourth rank tensor never gives rise to a six-fold anisotropic azimuthal pattern since the rank is less than 6. This explains why azimuthal pattern of Co/Ru superlattice in Fig. 2 is not anisotropic.

A slightly different experimental approach to characterize the MSHG response is to measure its polarization dependence with fixed input polarization. The dependence of the detected MSHG intensity on the analyzer angle ψ reveals (i) a shift by an angle $\delta\psi$ and (ii) variations of the maximum and minimum intensities upon magnetization reversal. Note that the latter is a fingerprint of the MSHG anisotropy since for isotropic surfaces in the longitudinal geometry only the angular shift has to be present [20]. These magnetization-induced effects can be described as follows. The polarization dependence $I_{2\omega}^{\alpha,\psi}(\varphi)$ of the MSHG intensity is given by

$$I_{2\omega}^{\alpha,\psi}(\varphi) = |E_{2\omega}^{\alpha,p}(\varphi, \pm M)\cos\psi + E_{2\omega}^{\alpha,s}(\varphi, \pm M)\sin\psi|^2 \quad (3)$$

where α denotes the incident fundamental polarization (α = s or p). The extrema of the $I_{2\omega}^{\alpha}(\psi)$ curve takes place at $\psi = \psi_{\pm}^{\alpha}$, which obey the condition

$$(|E_{2\omega}^{\alpha,p}(\varphi, \pm M)|^2 - |E_{2\omega}^{\alpha,s}(\varphi, \pm M)|^2)\tan 2\psi_{\pm}^{\alpha} = 2\mathrm{Re}[E_{2\omega}^{\alpha,p}(\varphi, \pm M)]E_{2\omega}^{\alpha,s}(\varphi, \pm M) \quad (4)$$

In analogy to linear magneto-optical Kerr effect, we introduce the nonlinear Kerr rotation angle as

$$\Theta_K^{(2)} = (\psi_+^{\alpha} - \psi_-^{\alpha})/2. \quad (5)$$

Fig. 4 shows the analyzer angle dependence of the SH intensity of the Fe(3.5 ML)/Au(3.5 ML) superlattice. Kerr rotation angle as determined by the Eq. (5) was 17.5°. Analyzer angle dependence of SHG intensity of Co(5 ML)/Ru(5 ML) for P polarization input was also measured. Very small nonlinear Kerr angle of 0.97° was obtained. The reduced value of nonlinear Kerr angle in Co/Ru superlattice may be due to the reduced value of linear Kerr angle in this superlattice, as well as due to its perpendicular anisotropy.

Table 1
Azimuthal amplitudes $A^{\alpha\beta}$, $B^{\alpha\beta}$, $C^{\alpha\beta}$ for samples with 3.5 ML

	$A^{\alpha\beta}$	$B^{\alpha\beta}$	$C^{\alpha\beta}$
P_{in}–P_{out}	130	4.0	11
S_{in}–P_{out}	46	2.7	9.0
P_{in}–S_{out}	33	3.6	1.7
S_{in}–S_{out}	12	6.9	0.95

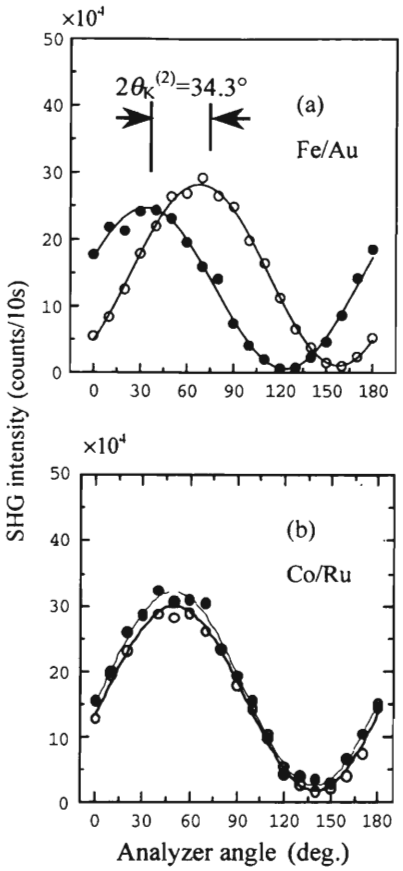

Fig. 4. Analyzer angle dependence of SHG intensity of (a) Fe(3.5 ML)/Au(3.5 ML) and (b) Co(5 ML)/Ru(5 ML) for S polarization input. Nonlinear Kerr rotation angle defined as a half of the phase difference between two opposite directions of magnetic field was 17.15° for the Fe/Au superlattice, while it was only 0.97° for the Co/Ru superlattice.

Theoretical analysis predicts that the Kerr angle depends on the azimuthal angle φ and also reveals a four-fold pattern in Fe/Au superlattice, which successfully explains the experimentally derived rotational dependence of the nonlinear Kerr angle.

In conclusion, we have shown that the MSHG response of Fe/Au(0 0 1) superlattices shows a strong azimuthal anisotropy on both the MSHG intensity as well as in the nonlinear magneto-optical Kerr rotation. These observations can fully be described by taking into account not only the interface-allowed dipole contributions but in addition the higher order (bulk-like) quadrupole contributions.

This work was supported in part by the Grant-in-Aid for Scientific Research in Priority Areas from Ministry of Education of Japan. We also express deep gratitude to European Community for our joint research.

References

[1] W. Hübner, K.-H. Bennemann, Phys. Rev. B 40 (1989) 5973.

[2] Th. Rasing, Nonlinear magneto-optics for magnetic thin films, in: O. Keller (Ed.), Notions and Perspectives of Nonlinear Optics, World Scientific Inc., Singapore, 1996, pp. 339–369.

[3] Th. Rasing, Nonlinear magneto-optical studies of ultrathin films and multilayers, in: K.H. Bennemann (Ed.), Nonlinear Optics of Metals, Oxford University Press, Oxford, 1997, pp. 132–218.

[4] H.A. Wierenga, M.W.J. Prins, D.L. Abraham, Th. Rasing, Phys. Rev. B 50 (1994) 1282.

[5] H.A. Wierenga, W. de Jong, M.W. Prins, Th. Rasing, R. Vollmer, A. Kirilyuk, H. Schwabe, J. Kirschner, Surf. Sci. 331–333 (1995) 1294.

[6] K. Takanashi, S. Mitani, M. Sato, H. Fujimori, H. Nakajima, A. Osawa, Appl. Phys. Lett. 67 (1995) 1016.

[7] S. Mitani, K. Takanashi, H. Nakajima, K. Sato, R. Schreiber, P. Grünberg, H. Fujimori, J. Magn. Magn. Mater. 156 (1996) 7.

[8] K. Sato, J. Abe, H. Ikekame, K. Takanashi, S. Mitani, H. Fujimori, J. Magn. Soc. Japan 20 (Suppl. S1) (1996) 35–40.

[9] K. Sato, E. Takeda, M. Akita, M. Yamaguchi, K. Takanashi, S. Mitani, H. Fujimori, Y. Suzuki, J. Appl. Phys. 86 (1999) 4985.

[10] S.S. Parkin, N. More, K.P. Roche, Phys. Rev. Lett. 64 (1990) 2304.

[11] M. Yamaguchi, K. Takanashi, K. Himi, K. Hayata, K. Sato, H. Fujimori, J. Magn. Magn. Mater., this issue.

[12] H. Nakazawa, S. Mitani, K. Takanashi, H. Nakajima, A. Osawa, H. Fujimori, J. Magn. Soc. Japan 20 (1996) 353 (in Japanese).

[13] K. Himi, K. Takanashi, S. Mitani, M. Yamaguchi, D.H. Ping, K. Hono, H. Fujimori, Appl. Phys. Lett. 78 (2001) 1436.

[14] K. Sato, A. Kodama, M. Miyamoto, K. Takanashi, H. Fujimori, Th. Rasing, J. Appl. Phys. 87 (2000) 6785.

[15] K. Sato, A. Kodama, M. Miyamoto, A.V. Petukhov, K. Takanashi, S. Mitani, H. Fujimori, Kirilyuk, Th. Rasing, Phys. Rev. B, submitted.

[16] R. Vollmer, M. Straub, J. Kirschner, Surf. Sci. 352 (1996) 684.

[17] D.A. Koos, V.L. Shanon, G.L. Richmond, Phys. Rev. B 47 (1993) 4730.

[18] K. Pedersen, O. Keller, J. Opt. Soc. Am. B 6 (1989) 2412.

[19] H.W.K. Tom, T.F. Heinz, Y.R. Shen, Phys. Rev. Lett. 51 (1983) 1983.

[20] Th. Rasing, M. Groot Koerkamp, B. Koopmas, H. van den Berg, J. Appl. Phys. 79 (1996) 6181.